Multinuclear Ag Clusters Sandwiched by Pt Complex Units: Fluxional Behavior and Chiral-at-Cluster Photoluminescence

Shinnosuke Horiuchi,* Sangjoon Moon, Akitaka Ito, Jacopo Tessarolo, Eri Sakuda, Yasuhiro Arikawa, Guido H. Clever, and Keisuke Umakoshi*

Abstract: *Multinuclear Ag clusters sandwiched by Pt complex units were synthesized and characterized by single crystal X-ray diffraction and NMR studies. The sandwich-shaped multinuclear Ag complexes showed two different types of fluxional behavior in solution: rapid slippage of Pt complex units on the Ag_3 core and a reversible demetalation–metalation reaction by the treatment with Cl anion and Ag ion, respectively. The Ag_2 complex obtained by demetalation reaction from the Ag_3 complex displayed U to Z isomerization. These multinuclear Ag complexes showed strong photoluminescence whose properties depended on the existence of Pt→Ag dative bonds. The Ag_3 complex, identified to be "chiral-at-cluster", was optically resolved by the formation of a diastereomeric salt with a chiral anion. The enantiomers show circular dichroism (CD) and circularly polarized luminescence (CPL) properties which is unprecedented for compounds based on a chiral sandwich structure. Theoretical calculations allow to understand their structural features and photophysical properties.*

Introduction

Multinuclear sandwich complexes, originating from extending the structural basis of the organometallic classic ferrocene $(C_5H_5)_2Fe$, have been intensively studied because of their fascinating structures and properties (Figure 1a).[1, 2] Such sandwich structures, which are generally symmetrical to the mirror plane defined by the sandwiched metal atoms, are stabilized by multiple metal–metal bonds and concerted coordination from their face-capping ligands. They often show fluxional behavior, such as dynamic rotation of the ligands,[1a, 1b, 1d, 1h] reversible metalation–demetalation sequences,[1e, 1q] and translocation of metal clusters,[1c, 1f, 1j] which represents a new horizon in cluster and materials chemistry. However, to the best of our knowledge, chiral multinuclear sandwich structures have not been reported.

Coinage d^{10} metal ions (Cu^I, Ag^I, Au^I) show strong metallophilic interactions to form metal clusters in the presence of suitable organic and inorganic ligands.[2, 3] In particular, pyrazolate ligands (pz) can bind three metal ions as side-capping ligands to give triangular M_3 complexes which show interesting luminescence properties.[4] These triangular M_3 complexes also provide a suitable platform to construct supramolecular 1D stacked structures in the solid state,[5] owing to the strong π–acidic/basic nature of the M_3 cores.[6]

These structural motifs motivated us to construct new types of sandwich-shaped multinuclear chiral complexes consisting of a coinage metal M_3 core and achiral face-capping ligands. We have reported a rare example of a square-planar Pt^{II} complex characterized as "chiral-at-metal" by using an achiral C^N chelating ligand.[7] We now extend this to "chiral-at-cluster" compounds, a concept that is arising from dissymmetry at a cluster core. When we employed phenyl-*N*-heterocyclic carbene (Ph-NHC) as a chelating ligand, followed by our synthetic procedure for heteropolynuclear metal complexes,[8] we have succeeded in the synthesis of sandwich-shaped multinuclear Ag complexes showing remarkable fluxional behavior and photoluminescence (Figure 1b). Very interestingly, these complexes have neither an inversion center nor a mirror plane in their complex cations, implying chirality. Herein we report the synthesis, characterization, and photoluminescence properties of multinuclear Ag clusters sandwiched by two Pt complex units. Multipoint coordination between Ag_3 cluster and Pt complex units endows them with a remarkable stability, enabling us to separate their enantiomers by formation of diastereomeric salts with a chiral anion. The chiral sandwich complexes allow us to observe chiroptical properties based on the sandwich structure for the first time.

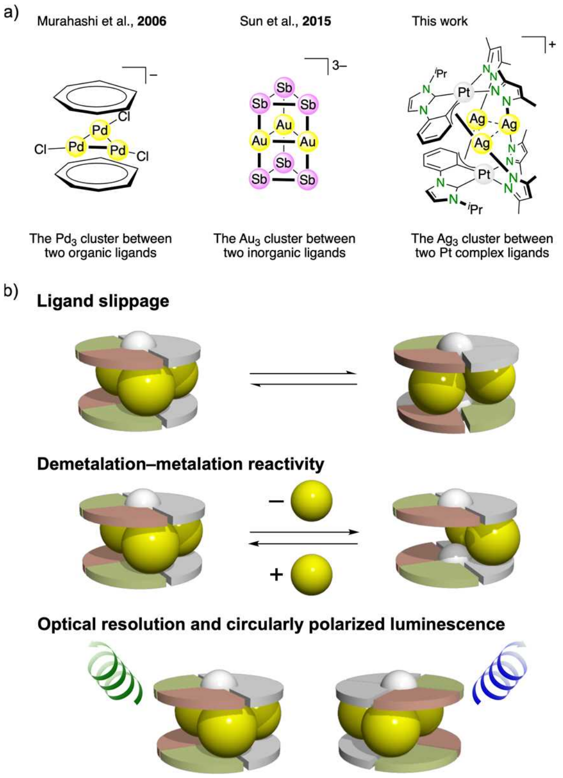

a) Murahashi et al., **2006** Sun et al., **2015** This work

The Pd_3 cluster between two organic ligands

The Au_3 cluster between two inorganic ligands

The Ag_3 cluster between two Pt complex ligands

b) **Ligand slippage**

Demetalation–metalation reactivity

Optical resolution and circularly polarized luminescence

---

[*] Dr. S. Horiuchi, Dr. S. Moon, Dr. E. Sakuda, Dr. Y. Arikawa, Prof. Dr. K. Umakoshi
Division of Chemistry and Materials Science, Graduate School of Engineering, Nagasaki University
1-14, Bunkyo-machi, Nagasaki 852-8521 (Japan)
E-mail: kumks@nagasaki-u.ac.jp

Dr. A. Ito
School of Environmental Science and Engineering, Graduate School of Engineering, Kochi University of Technology
185 Miyanokuchi, Tosayamada, Kami, Kochi 782-8502 (Japan)

Dr. S. Horiuchi, Dr. E. Sakuda, Dr. J. Tessarolo, Prof. Dr. G. H. Clever
Department of Chemistry and Chemical Biology
TU Dortmund University
Otto-Hahn-Straße 6, 44227 Dortmund (Germany)

Supporting information and ORCID identification number(s) for the author(s) of this article can be found under: https://doi.org/10.1002/anie. 202101460.

Figure 1. a) Sandwich-shaped metal clusters. b) Fluxional behavior and chiral-at-cluster photoluminescence of the sandwich-shaped Ag_3 cluster.

Results and Discussion

Sandwich-shaped multinuclear Ag_3 complex [**2a**]BF_4 was prepared in a one step reaction from mononuclear Pt complex [**1a**]Cl with $AgBF_4$ (2.5 eq.) in the presence of base (Figure 2). The formation of [**2a**]BF_4 was confirmed by elemental analysis and electro-spray ionization (ESI) mass spectrometry, whose signal was observed at *m*/*z* 1465.6, corresponding to [**2a**]$^+$. The molecular structure of [**2a**]BF_4 was undoubtedly revealed by single crystal X-ray analysis. A yellow crystal of [**2a**]BF_4 was obtained from CH_2Cl_2/*n*-pentane solution. The structure of [**2a**]BF_4 shows that the Ag_3 core is sandwiched between two Pt complex units. All Ag ions form a linear coordination geometry (Figure 2b). The intramolecular Ag···Ag distances in [**2a**]$^+$ (Ag1···Ag3: 3.0099(9), Ag2···Ag3: 3.0144(10) and Ag1···Ag2: 3.2906(9) Å) are considerably shorter than those of trinuclear Ag(I) pyrazolato complexes (3.296–3.702 Å),[4] suggesting that the Ag ions in [**2a**]BF_4 strongly adhere to each other via argentophilic interactions.[3b] One Ag(I) ion (Ag3) was found to be coordinated by two pyrazolato ligands, whereas the other two Ag(I) ions (Ag1 and Ag2) are supported by the coordination of two Pt complex units, that is, pyrazolato ligands, dative bonds from Pt atoms (Pt1···Ag1: 2.8400(7), Pt1···Ag2: 3.0774(8), Pt2···Ag1: 3.1372(8), and Pt2···Ag2: 2.8187(8) Å) and π-coordination of a phenyl moiety (Ag–π interaction). These interactions seem to concertedly stabilize the multinuclear sandwich framework. The flexibility arising from the multiple-point coordination modes of Ag1 and Ag2 probably contribute to the observed shrinking of the Ag_3 core sandwiched by the two Pt complex units. It is noted that the structure of the Pt_2Ag_3 framework in [**2a**]$^+$ is considerably differing from a similar Pt_2Ag_3 systems containing phenylpyridinato (ppy) and rollover bipyridinato (bpy*) chelating ligands as reported in our previous paper.[8b,8d] There, those structures contained one Ag(I) ion trapped by two dative bonds from Pt metal centers and two Ag(I) ions coordinated by two pyrazolato ligands (Figure S19).

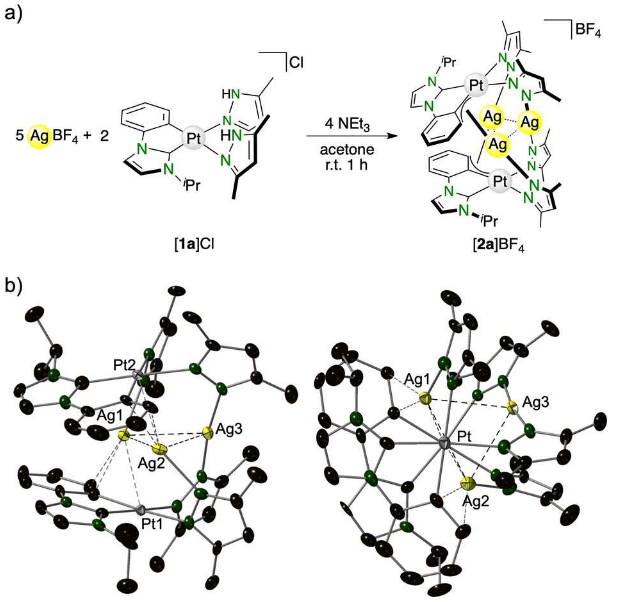

Figure 2. a) Synthesis of multinuclear Ag_3 sandwich complex [**2a**]BF_4 and b) X-ray structure of [**2a**]$^+$ with the atom numbering scheme (50% probability ellipsoids): (left) side view, (right) viewed along the Pt•••Pt axis. Hydrogen atoms and the BF_4 anion are omitted for clarity.

Interestingly, the Ag_3 sandwich complex showed remarkable fluxional behavior in solution, though multiple-point coordination of the two Pt complex units toward the Ag_3 core were observed in the crystalline state. The ^{1}H NMR spectrum of [**2a**]BF_4 recorded in $CDCl_3$ (30 mM) showed one set of signals (coalescence) at 30 ºC, which clearly split into two sets of signals at –50 ºC (Figure 3). A variable temperature (VT) ^{195}Pt NMR spectrum also showed one doublet at –3247 ppm ($^1J(^{195}Pt–^{107,109}Ag)$ = 480 Hz) at 30 ºC and two doublets at –3275 ppm ($^1J(^{195}Pt–^{107,109}Ag)$ = 528 Hz) and –3279 ppm ($^1J(^{195}Pt–^{107,109}Ag)$ = 682 Hz) at –50 ºC (Figure S20). These results indicate that intramolecular isomerization of [**2a**]$^+$ took place in solution, as also supported by the 2D ^{1}H–^{1}H EXchange SpectroscopY (EXSY) experiments recorded at –50 ºC (Figure S22).

Since several attempts to obtain single crystals of the stereoisomer, [**2a'**]$^+$ (Figure 3a), were not successful, the structure of [**2a'**]$^+$ was characterized by NMR spectroscopy at low temperature. As compared with the signal at 6.23 ppm, assigned to the phenyl moieties' ortho-proton (relative to the Pt(II) ion; marked with "*a*") of the Ph-NHC ligand in [**1a**]$^+$, the corresponding signals of the Pt_2Ag_3 complex at –50 ºC significantly shifted, as they were observed at 5.67 (Δδ = –0.6 ppm) and 6.87 ppm (Δδ = +0.6 ppm), respectively (Figure 3c, d). According to our previous studies concerning the formation of Pt_2Ag_3 complexes, the signal of the ortho-proton "*a*" showed a large up-field shift after formation of a Pt_2Ag_3 framework in which one of the three Ag(I) ions was trapped by two Pt→Ag dative bonds and the remaining two Ag(I) ions were coordinated by two pyrazolato ligands, respectively (Figure S19).[8b,8d] These results suggest that the signal observed at 5.67 ppm can be assigned to the ortho-proton of [**2a'**]$^+$, and thus the low magnetic field side signal at 6.87 ppm can be assigned to [**2a**]$^+$, whose structure was clearly determined by X-ray crystallographic analysis in this study (Figure 2). Thus, [**2a**]$^+$

showed a rapid twisting motion of the coordination plane on the Ag$_3$ core to form the structural isomer [**2a’**]$^+$ in solution. Similar down-field shift in a ^{1}H NMR spectrum was also observed for the π-coordination of a carbon-carbon double bond to an acidic Ag(I) ion.[9]

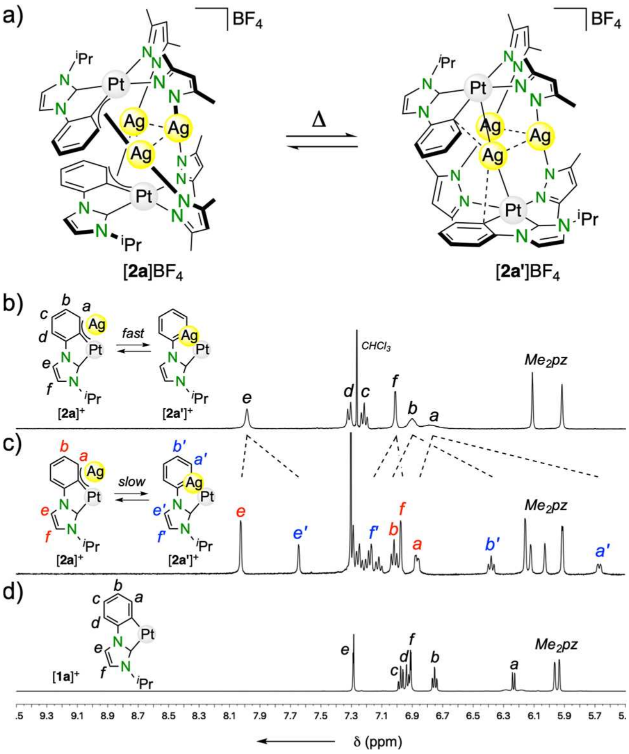

Figure 3. a) Schematic representation of the isomerization between [**2a**]$^+$ and [**2a’**]$^+$. b-d) ^{1}H NMR spectra (400 M Hz, CDCl$_3$) of the Ag$_3$ sandwich complex recorded at b) 303 K and c) 223 K, and d) mononuclear Pt complex [**1a**]Cl at 303 K.

Notably, according to the integral ratio determined from the ^{1}H NMR spectrum, the ratio of structural isomers in the Ag$_3$ sandwich complex is [**2a**]$^+$:[**2a’**]$^+$ = 2:1 at –50 ºC, indicating that [**2a**]$^+$ is 1.3 kJ/mol more stable thermodynamically than [**2a’**]$^+$ at –50 ºC (Figure 3c). The different coordination modes of the Pt complex units toward the Ag$_3$ core affect the thermodynamic stability of each isomer of the sandwich complex in solution. The kinetic and activation parameters for the isomerization between [**2a**]$^+$ and [**2a’**]$^+$ were estimated by line-shape and Eyring analyses ($\Delta H^{\ddagger}$ = 53.5 ± 1.0 kJ mol^{-1}, $\Delta S^{\ddagger}$ = 3.8 ± 3.7 J mol^{-1} K^{-1}, Figures S39–40, Table S1). These parameters clearly explain that the isomerization is an enthalpy-controlled process in a unimolecular fashion. The high activation enthalpy ($\Delta H^{\ddagger}$) stems from the multiple bond recombinations between the Ag$_3$ core and Pt complex units during the isomerization.

The flexibility of [**2a**]BF$_4$ in the solid state was examined by ^{13}C cross-polarization/magic angle spinning (CP/MAS) NMR measurements. The ^{13}C CP/MAS NMR spectrum of single crystals of [**2a**]BF$_4$ showed two sets of signals corresponding to the Pt complexes units (Figure S23). Considering the structure of [**2a**]$^+$ with C_1 symmetry due to the nonequivalence of the Pt complex units in the crystalline state, the observation of two sets of signals in the ^{13}C CP/MAS NMR spectrum indicates that the isomerization between [**2a**]$^+$ and [**2a’**]$^+$ is suppressed in the crystalline state. The close packing of the complex salt in the solid thus seems to suppress the fluxional nature of [**2a**]$^+$.

The fluxionality of the Ag$_3$ cluster in solution strongly depends on the steric bulkiness of the bridging pyrazolato ligands and electronic nature of the chelating ligand on the Pt complex units. When sterically demanding 3,5-diphenylprazolato (Ph$_2$pz) ligands were introduced to the sandwich-shaped Ag$_3$ cluster instead of 3,5-dimethylprazolato (Me$_2$pz) ligands, a corresponding Pt$_2$Ag$_3$ complex [**2b**]BF$_4$ was formed in a similar synthetic manner, whose structure was mostly identical to that of [**2a**]BF$_4$, as confirmed by X-ray crystallographic analysis (Figure S54). However, the ^{1}H NMR spectrum of [**2b**]$^+$ did not change significantly at elevated temperatures, indicating that the Pt$_2$Ag$_3$ complex having Ph$_2$pz bridging ligands did not show the isomerization as observed for [**2a**]$^+$ (Figure S30). The bulky phenyl groups on the pyrazolato ligands may sterically control the rigidity of the Pt$_2$Ag$_3$ framework and prevent bond recombinations between the Ag$_3$ core and the Pt complex units, resulting in the effective inhibition of the thermal slippage of Pt complex units on the Ag$_3$ core. The Pt$_2$Ag$_3$ complex having ppy chelating ligands and Me$_2$pz bridging ligands, which was reported in our previous paper,[8b] also did not show similar structural isomerization as confirmed by the VT NMR study (Figure S19).

Computational studies revealed the origin of the fluxional nature of [**2a’**]$^+$, leading to the formation of structural isomer [**2a**]$^+$. The Mayer bond indices of the Me$_2$pz bridged Pt$_2$Ag$_3$ complexes, whose structures were optimized by DFT calculations, showed that both the Pt→Ag dative and Ag–C(ipso) bonds in the Ph-NHC complex [**2a’**]$^+$ are weaker than those of ppy analogue (Table S24).[10] These results suggest that the weak π-acidic nature of the NHC moiety in [**2a’**]$^+$ effectively weakens the Pt→Ag dative bond and π-coordination ability of the ipso-carbon atom, endowing the flexibility in the Ag$_3$ core.[11] The comparable Ag–Ag bonding nature in [**2a’**]$^+$ also contributed to bring out the stability and the fluxional nature of the Ag$_3$ core, as compared with the ppy system.

The Ag$_3$ core showed a reversible demetalation–metalation reactivity. Multinuclear Ag$_3$ sandwich complex [**2a**]BF$_4$ reacted with Cl anion to afford the corresponding Ag$_2$ sandwich complex **3a** in 50% isolated yield, whose structure was clearly revealed by X-ray crystallographic analysis (Figure 4). The Ag$_2$ cluster was supported by only pyrazolato ligands and argentophilic interaction between the Ag ions (Ag1···Ag2: 2.9384(6) Å), forming U-shaped Pt$_2$Ag$_2$ structure **3a**$_{\text{U}}$.[12, 13] The ^{195}Pt NMR spectrum showed a sharp singlet signal at –3727 ppm, indicating that the Pt–Ag interactions were negligible in the Ag$_2$ structure (Figure S37). The Pt$_2$Ag$_2$ framework can subsequently incorporate a Ag(I) ion within the U-shaped cavity to regenerate [**2a**]$^+$ quantitatively (Figure S41).

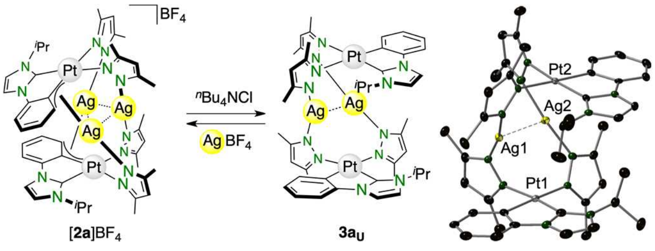

Figure 4. Reversible metalation–demetalation reactivities of the multinuclear sandwich complexes and X-ray structure of **3a$_U$** with the atom numbering scheme (50% probability ellipsoids). Hydrogen atoms are omitted for clarity.

Considering the metalation process of **3a**, the U-shaped Pt_2Ag_2 complex **3a$_U$** seems to be a reaction intermediate in the formation of the sandwich-type Ag_3 cluster from [**1a**]Cl (Figure 2). Thus, we carefully monitored the reaction of [**1a**]Cl with Ag(I) ions ($AgBF_4$, 2 eq.) in the presence of NEt_3. Although the Pt_2Ag_2 complex **3a** exists as a mixture of U- and Z-shaped isomers in solution (*vide infra*), the ^{1}H NMR spectrum of the reaction mixture interestingly showed that it contained [**1a**]$^+$ and [**2a**]$^+$ in a 1:1 ratio rather than the Pt_2Ag_2 complex (Figure S42). Additionally, when a Ag(I) ion was added to the mixture of Pt complex [**1a**]BF_4 and Pt_2Ag_2 complex **3a** in a 1:1 ratio in the presence of NEt_3, the Ag(I) ion smoothly reacted with **3a** to afford the Pt_2Ag_3 complex [**2a**]$^+$ without consuming [**1a**]$^+$ (Figure S43). These observations revealed that the reactivity of the Pt_2Ag_2 complex toward Ag(I) ion is much higher than that of the mononuclear Pt complex, and this is the reason why the reaction of **1a** with Ag(I) ion gave **3a** directly. This is one of the rare examples of a host-guest complex which encapsulates an additional Ag(I) ion in its cavity.[14]

The sandwich Ag_2 complex **3a$_U$** also showed a fluxional behavior whose type is different from that of [**2a**]$^+$ in solution. When single crystals of the U-shaped Pt_2Ag_2 complex **3a$_U$** were dissolved in $CDCl_3$, new sets of signals appeared and their intensities gradually increased in the ^{1}H NMR spectrum, suggesting the occurrence of U to Z isomerization of the Pt_2Ag_2 complex (Figure S44).[8c, 8d] The isomerization reached U : Z = 1:1 ratio in a thermodynamic equilibrium state within 1 h even in highly diluted solution (60 μM), showing that the reaction rate of the U to Z isomerization of the neutral Pt_2Ag_2 complex **3a$_U$** is faster than that of the cationic Pt_2Ag_2 complex having pyridyl-NHC chelating ligands.[8c] Although the reaction mechanism of the U to Z isomerization is still unclear, this isomerization might proceed in an intermolecular fashion and the rate acceleration might originate from the fluxionality of the sandwich framework featuring Ph-NHC chelating ligands and no charge of the complex: hence, the neutral Pt_2Ag_2 complexes having Ph-NHC chelating ligands can easily access each other to undergo rapid intermolecular pyrazolate–Ag–pyrazolate bond recombination, while the dicationic Pt_2Ag_2 complexes having pyridyl-NHC chelating ligands are electrostatically more repulsive as shown in our previous study.[8c]

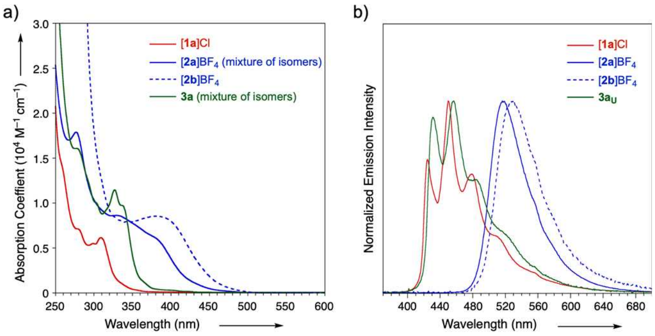

Figure 5. a) Absorption spectra (in CH_2Cl_2, r.t.) and b) emission spectra in the crystalline states (λ_{ex} = 355 nm).

We next investigated the photophysical properties of the sandwich complexes as metal–metal interactions were expected to contribute significantly (Figure 5).[15] The Pt complex unit [**1a**]$^+$ in CH_2Cl_2 solution (10 μM) showed the lowest energy absorption band at 315 nm ascribed to the ligand-to-metal charge-transfer (LMCT) [π(Ph-NHC) → Pt] transitions mixed with the intraligand charge transfer (ILCT) [π(Ph-NHC) → π*(Ph-NHC)] transitions and d-d transitions, as revealed by TD-DFT calculations (Tables S8–S10, Figure S56). After formation of the Ag_3 sandwich structure, the absorption band red-shifted to 400 nm,[16] owing to the formation of Pt→Ag dative bonds (metal-metal interactions). The TD-DFT calculations for [**2a**]$^+$ clearly showed that the molecular orbitals around the Ag_3 cluster contributed to the electronic transitions in addition to the original transitions of the Pt complex units. The lowest energy absorption bands of [**2a**]$^+$ can be mainly assigned to the charge transfer transition from the Me_2pz bridging ligand to the Pt_2Ag_3(Ph-NHC)$_2$ moiety, a LMM'L'CT [Me_2pz → Pt/Ag/π*(Ph-NHC)] transition, which is similar to the assignment for Pt_2Ag_3 complex having ppy chelating ligands (Tables S11–S13, Figure S57).[8b] After formation of the Ag_2 sandwich structure by demetalation of the Ag_3 complex, the lowest energy absorption bands were blue-shifted owing to the disappearance of Pt→Ag dative bonds. The TD-DFT calculations for **3a$_U$** also supported that the atomic orbitals around Ag ions participated little in the electronic transitions regarding the lowest energy absorption band, which can be mainly assigned to the combination of the ligand-to-ligand charge-transfer (LL'CT) [Me_2pz → π*(Ph-NHC)], metal-to-ligand charge-transfer (MLCT) [Pt → π*(Ph-NHC)] and ILCT [π(Ph-NHC) → π*(Ph-NHC)] transitions (Table S20–S22, Figure S60). Thus, the photophysical properties of the sandwich-type multinuclear Ag complexes depend on the presence of Pt→Ag dative bonds, which is also obvious in their emission properties (Figure 6).

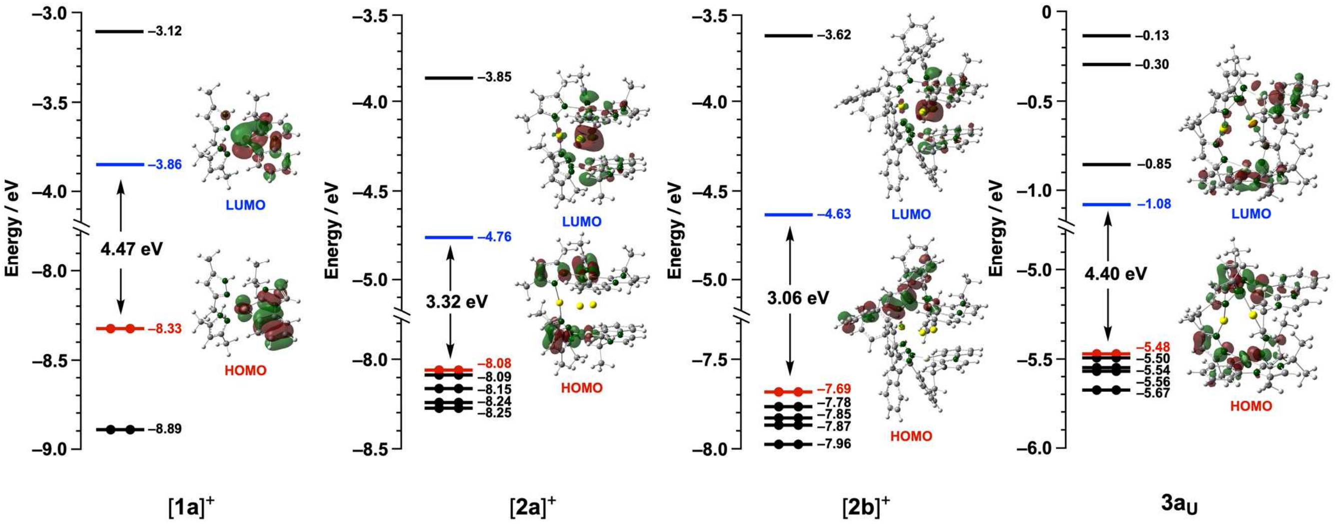

Figure 6. Energy diagram showing the energy values of the frontier Kohn–Sham molecular orbitals of [**1a**]$^+$, [**2a**]$^+$, [**2b**]$^+$, and **3a$_U$** in gas phase. HOMOs and LUMOs of the complexes are also displayed (isovalue = 0.04).

The sandwich complexes showed intense photoluminescence in the crystalline state (Figure 5b, Table S3). Single crystals of Ag$_3$ sandwich complex [**2a**]BF$_4$ showed a broad emission spectrum (λ_{max} = 517 nm, Φ = 46%), whereas the Ag$_2$ sandwich complex **3a$_U$** displayed a structured one (λ_{max} = 457 nm, Φ = 22%) similarly to that of Pt complex unit [**1a**]Cl (λ_{max} = 450 nm, Φ = 72%). Time-resolved lifetime measurements revealed that the emission lifetimes of sandwich complexes [**2a**]$^+$ and **3a$_U$** were comparable to each other in the microsecond regime, indicating that the emissions originated from their triplet states (phosphorescence). It is noted that the photoluminescence properties of the mixture of stereoisomers of Pt$_2$Ag$_3$ complex, [**2a**]BF$_4$ and [**2a'**]BF$_4$, in the solid state were almost identical to that of the crystalline sample of pure [**2a**]BF$_4$ (Figure S49). It suggests that the coordination mode between the Ag$_3$ core and the Pt complex units does not affect their photophysical properties, significantly. The emission intensities of Pt$_2$Ag$_3$ and Pt$_2$Ag$_2$ complexes drastically decrease in solution owing to the fluxional behavior of the sandwich-shaped multinuclear Ag clusters (Table S2). In particular, the more sterically hindered sandwich complex [**2b**]BF$_4$ showed a brighter luminescence (λ_{max} = 529 nm, Φ = 12%) than the flexible sandwich complex [**2a**]BF$_4$ (λ_{max} = 529 nm, Φ = 3%) in solution (Table S2, Figure S47b).

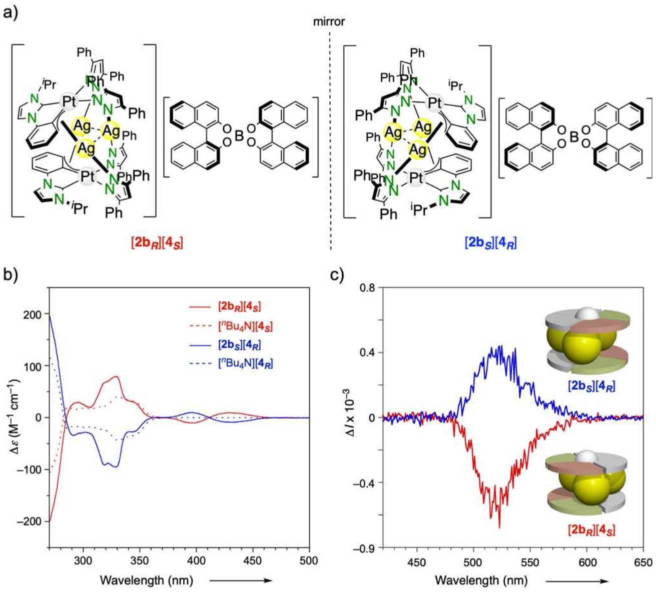

Figure 7. a) Schematic representation of the enantiomeric salts [**2b$_R$**][**4$_S$**] and [**2b$_S$**][**4$_R$**]. b) Circular dichroism (CD) spectra (10 μM, CH$_2$Cl$_2$, r.t.) of enantiomerically pure Ag$_3$ sandwich complexes [**2b**][**4**] ([**2b$_R$**][**4$_S$**] and [**2b$_S$**][**4$_R$**], solid line) and the chiral BINOL salt [^{n}Bu$_4$N][**4**] (broken line). c) Circularly polarized luminescence (CPL) spectra (75 μM, CH$_2$Cl$_2$, λ_{ex} = 350 nm) of [**2b**][**4**] after optical resolution.

The Pt complex units exhibit planar chirality after construction of the sandwich structure,[17] resulting in the generation of dissymmetry at the Pt$_2$Ag$_3$ cluster. In particular, as the slippage of Pt complex unit in [**2a**]BF$_4$ proceeded via an intramolecular fashion even at elevated temperature, owing to the multipoint coordination between the Ag$_3$ core and the Pt complex units, the absolute configurations of the sandwich structures would maintain and not show racemization in solution. Thus ^{1}H NMR signals of the metal cluster split into two sets of signals by addition of chiral anions, owing to the formation of diastereomeric salts (Figure S46). Because solubility of the diastereomeric salts differs, the diastereomerically pure

Pt_2Ag_3 complexes (based on the ^1H NMR spectrum) were slowly precipitated as a powder by a diffusion of hexane vapor into the acetone solution of [**2b**]BF_4 in the presence of 5 equivalents of sodium bis-(*S*)- and (*R*)-BINOL borate (Na[**4**$_S$] and Na[**4**$_R$]) as chiral anion, respectively (Figure S45).[18,19] The circular dichroism (CD) spectra recorded for solutions of both enantiomeric salts in CH_2Cl_2 clearly showed Cotton effects originated from the chiral Ag_3 complex at 387 and 430 nm (Figure 7a,b). The absolute configurations of the Pt_2Ag_3 complex cations in the isolated diastereomers could be proposed on the basis of TD-DFT calculations of electronic circular dichroism (ECD) spectra, suggesting that the isolated diastereomers were [**2b**$_R$][**4**$_S$] and [**2b**$_S$][**4**$_R$], respectively (Figure S61).

The optical resolution of the sandwich-shaped Ag_3 cluster enabled us to conduct a circularly polarized luminescence (CPL) study.[7,20] The CPL spectra of the enantiomers in degassed CH_2Cl_2 upon excitation at 350 nm clearly showed relatively intense opposite polarization of emitted light for both optically resolved complexes (Figure 7c). The luminescence of [**2b**$_R$][**4**$_S$] and [**2b**$_S$][**4**$_R$] at 529 nm show right- and left-handed CPL, respectively, whose luminescence dissymmetry factor g_{lum} was 1.8×10^{-3}. Although the g_{lum} value is comparable to that of a reported chiral Ag nano cluster,[21] it should be noted that, to our best knowledge, this is the first example for observing the CPL property from multinuclear sandwich-shaped metal complexes. The multipoint coordination between the Ag_3 cluster and the Pt complex units provides the required stability to the Pt_2Ag_3 sandwich structure for allowing optical resolution.

Conclusion

Herein, we have revealed that multinuclear Ag complexes sandwiched by two Pt complex units show two different types of dynamic behavior in solution and remarkable photoluminescence properties. The Ag_3 complexes feature rapid thermal slippage of Pt complex units on the Ag_3 core and reversible metalation–demetalation reactivity. The photophysical properties were altered by the presence of Pt→Ag dative bonds. Furthermore, the formation of a sandwich-shape structure provided planar chirality at the Pt complex units, allowing the separation of their enantiomeric salts using a chiral counter anion, which showed circular dichroism and circularly polarized luminescence. The origins of these structural and photophysical properties in the sandwich-shaped multinuclear Ag clusters were revealed by DFT calculations. These results extend structural concepts of multinuclear sandwich complexes and give impulses for the development of novel chiral luminescent materials based on sandwich-shaped multinuclear complexes.

Acknowledgements

This research was financially supported by JSPS KAKENHI Grant Numbers JP16H0659, JP19K15589, JP19H04587, JP20K05542, and JP20H05231, by Izumi Science and Technology Foundation, and by the precious metals research grants from TANAKA memorial foundation. S.H. and E.S. thank the JSPS program for Advancing Strategic International Networks to Accelerate the Circulation of Talented Researchers. This work was a result of using research equipment shared in MEXT project for promoting public utilization of advanced research infrastructure (Program for supporting introduction of the new sharing system) Grant Number JPMXS0422500320. This work was funded by the Deutsche Forschungsgemeinschaft (DFG) under Germany's Excellence Strategy – EXC 2033 – 390677874 – RESOLV. S.M. thanks Rotary Yoneyama Memorial Foundation and Rotary Club of Nagasaki North Founding for a PhD fellowship. We thank Dr. Tsutomu Fukuda and Dr. Thorben R. Schulte for helpful discussion. We are grateful to J. Nagaoka for the X-ray measurements.

Conflict of interest

The authors declare no conflict of interest.

Keywords: Sandwich complex • Ag cluster • photoluminescence • fluxional behavior • Pt complex

[1] a) T. Murahashi, M. Fujimoto, M. Oka, Y. Hashimoto, T. Uemura, Y. Tatsumi, Y. Nakao, A. Ikeda, S. Sakaki, H. Kurosawa, *Science* **2006**, *313*, 1104-1107; b) T. Murahashi, R. Inoue, K. Usui, S. Ogoshi, *J. Am. Chem. Soc*. **2009**, *131*, 9888-9889; c) T. Murahashi, K. Shirato, A. Fukushima, K. Takase, T. Suenobu, S. Fukuzumi, S. Ogoshi, H. Kurosawa, *Nature Chem*. **2011**, *4*, 52-58; d) T. Murahashi, K. Usui, R. Inoue, S. Ogoshi, H. Kurosawa, *Chem. Sci*. **2011**, *2*, 117-122; e) S. Horiuchi, Y. Tachibana, M. Yamashita, K. Yamamoto, K. Masai, K. Takase, T. Matsutani, S. Kawamata, Y. Kurashige, T. Yanai, T. Murahashi, *Nature Commun*. **2015**, *6*, 6742; f) K. Masai, K. Shirato, K. Yamamoto, Y. Kurashige, T. Murahashi, *Chem. Commun*. **2016**, *52*, 6427-6430; g) Y. Ishikawa, K. Yamamoto, T. Murahashi, *Angew. Chem. Int. Ed*. **2017**, *56*, 1346-1350; h) M. Teramoto, K. Iwata, H. Yamaura, K. Kurashima, K. Miyazawa, Y. Kurashige, K. Yamamoto, T. Murahashi, *J. Am. Chem. Soc*. **2018**, *140*, 12682-12686; i) M. Yamashita, Y. Kawasumi, Y. Tachibana, S. Horiuchi, K. Yamamoto, T. Murahashi, *Chem. Eur. J*. **2019**, *25*, 1212-1216; j) M. Yamashita, S. Horiuchi, K. Yamamoto, T. Murahashi, *Dalton. Trans*. **2019**, 48, 13149-13153; k) T. Ishikawa, A. Kawamura, T. Sugawa, R. Moridaira, K. Yamamoto, T. Murahashi, *Angew. Chem. Int. Ed*. **2019**, *58*, 15318-15323; l) L.-J. Wang, X. Li, S. Bai, Y.-Y. Wang, Y.-F. Han, *J. Am. Chem. Soc*. **2020**, *142*, 2524-2531.

[2] F.-X. Pan, L.-J. Li, Y.-J. Wang, J.-C. Guo, H.-J. Zhai, L. Xu, Z.-M. Sun, *J. Am. Chem. Soc*. **2015**, *137*, 10954-10957.

[3] For selected reviews of metallophilic interactions, see: a) H. Schmidbaur, A. Schier, *Chem. Soc. Rev*. **2012**, *41*, 370-412; b) H. Schmidbaur, A. Schier, *Angew. Chem. Int. Ed*. **2015**, *54*, 746-784; c) N. V. S. Harisomayajula, S. Makovetskyi, Y.-C. Tsai, *Chem. Eur. J*. **2019**, *25*, 8936-8954.

[4] For selected reviews of triangular M_3 complexes, see: a) K. Fujisawa, Y. Ishikawa, Y. Miyashita, K. Okamoto, *Inorg. Chim. Acta*. **2010**, *363*, 2977-2989; b) Y. Morishima, D. J. Young, K. Fujisawa, *Dalton Trans*. **2014**, *43*, 15915-15928; c) J. Zheng, Z. Lu, K. Wu, G.-H. Ning, D. Li, *Chem. Rev*. **2020**, *120*, 9675–9742.

[5] a) M. A. Omary, A. A. Mohamed, M. A. Rawashdeh-Omary, J. P. Fackler Jr., *Coord. Chem. Rev*. **2005**, *249*, 1372-1381; b) M. A. Omary, M. A. Rawashdeh-Omary, M. W. A. Gonser, O. Elbjeirami, T. Grimes, T. R. Cundari, *Inorg. Chem*. **2005**, *44*, 8200-8210; c) H. V. R. Dias, C. S. P. Gamage, *Angew. Chem. Int. Ed*. **2007**, *46*, 2192-2194; d) M. A. Rawashdeh-Omary, M. D. Rashdan, S. Dharanipathi, O. Elbjeirami, P. Ramesh, H. V. R. Dias, *Chem. Commun*. **2011**, *47*, 1160-1162; e) N. B. Jayaratna, C. V. Hettiarachchi, M. Yousufuddin, H. V. R. Dias, *New J. Chem*. **2015**, *39*, 5092-5095; f) N. B. Jayaratna, M. M. Olmstead, B. I. Kharisov, H. V. R. Dias, *Inorg. Chem*. **2016**, *55*, 8277-8280; f) R. Hahn, F. Bohle, S. Kotte, T. J. Keller, S.-S. Jester, A. Hansen, S. Grimme, B. Esser, *Chem. Sci*. **2018**, *9*, 3477-3483; g) R. Hahn, F. Bohle, W. Fang, A. Walther, S. Grimme, V. Esser, *J. Am. Chem. Soc*. **2018**, *140*, 17932-17944.

[6] S. M. Tekarli, T. R. Cundari, M. A. Omary, *J. Am. Chem. Soc*. **2008**, *130*, 1669-1675.

[7] T. R. Schulte, J. J. Holstein, L. Krause, R. Michel, D. Stalke, E. Sakuda, K. Umakoshi, G. Longhi, S. Abbate, G. H. Clever, *J. Am. Chem. Soc*. **2017**, *139*, 6863-6866.

[8] a) K. Nishihara, M. Ueda, A. Higashitani, Y. Nakao, Y. Arikawa, S. Horiuchi, E. Sakuda, K. Umakoshi, *Dalton Trans*. **2016**, *45*, 4978-4982; b) M. Ueda, S. Horiuchi, E. Sakuda, Y. Nakao, Y. Arikawa, K. Umakoshi, *Chem. Commun.*

2017, *53*, 6405-6408; c) S. Horiuchi, S. Moon, E. Sakuda, A. Ito, Y. Arikawa, K. Umakoshi, *Dalton Trans*. **2018**, *47*, 7113-7117; d) S. Horiuchi, S. Tanaka, S. Moon, E. Sakuda, A. Ito, Y. Arikawa, K. Umakoshi, *Inorg. Chem*, **2021**, *60*, 1513-1522; e) S. Horiuchi, K. Umakoshi, *Chem. Rec*. **2021**, DOI: 10.1002/tcr.202000125.

[9] a) M. Munakata, L. P. Wu, G. L. Ning, *Coord. Chem. Rev.* **2000**, *198*, 171-203; b) H. V. R. Dias, M. Fianchini, T. R. Cundari, C. F. Campana, *Angew. Chem. Int. Ed*. **2008**, *47*, 556-559; c) M. Fianchini, H. Dai, H. V. R. Dias, *Chem. Commun*. **2009**, *45*, 6373-6375; d) S. A. Baudron, *Coord. Chem. Rev.* **2019**, *380*, 318-329; e) M. F. Ibad, A. Schulz, A. Villinger, *Organometallics* **2019**, *38*, 1445-1458.

[10] The Mayer bond indices were calculated on a Multiwfn program, see: T. Lu, F. Chen, *J. Comput. Chem*., **2012**, *33*, 580-592.

[11] a) O. Back, M. H.-Ellinger, C. D. Martin, D. Martin, G. Bertrand, *Angew. Chem. Int. Ed*. **2013**, *52*, 2939-2943; b) D. J. Nelson, S. P. Nolan, *Chem. Soc. Rev*. **2013**, *42*, 6723-6753; c) H. V. Huynh, *Chem. Rev*. **2018**, *118*, 9457-9492.

[12] The crude reaction mixture after the demetalation reaction included both U- and Z-shaped isomers of **3a**. The solubility of **3a**$_{\mathrm{U}}$ was significantly lower than that of **3a**$_{\mathrm{Z}}$, resulted in the selective crystallization of **3a**$_{\mathrm{U}}$ from the mixture.

[13] Pt_2 and Pt_2Ag_2 complexes having cyclometallated NHC chelating ligands and Me_2pz bridging ligands have been reported, see: a) P. Pinter, Y. Unger, T. Strassner, *ChemPhotoChem*, **2017**, *1*, 113-115; b) L. Arnal, S. Fuertes, A. Martin, V. Sicilia, *Chem. Eur. J*. **2018**, *24*, 9377-9384.

[14] a) T. Osuga, T. Murase, M. Fujita, *Angew. Chem. Int. Ed*. **2012**, *51*, 12199-12201; b) Y. Kohyama, T. Murase, M. Fujita, *Angew. Chem. Int. Ed*. **2014**, *53*, 11510-11513; c) A. Vellé, A. Cebollada, M. Iglesias, P. J. Sanz Miguel, *Inorg. Chem.* 2014, 53, 10654-10659; d) B. Hua, L. Shao, Z. Zhang, J. Liu, F. Huang, *J. Am. Chem. Soc*. **2019**, *141*, 15008-15012.

[15] Metal-metal interactions typically altered their emission properties of the complexes. For selected reviews, see: a) V. W.-W. Yam, V. K.-M. Au, S. Y.-L. Leung, *Chem. Rev*. **2015**, *115*, 7589-7728; b) H. B. Gray, S. Záliš, A. Vlček, *Coord. Chem. Rev*. **2017**, *345*, 297–317; c) M. Yoshida, M. Kato, *Coord. Chem. Rev*. **2018**, *355*, 101-115.

[16] The absorption spectra recorded in CH_2Cl_2 solutions derived from the mixture of isomers because of the rapid isomerization of the sandwich complexes.

[17] For selected reviews of planer chirality, see: a) Z. Hassan, E. Spuling, D. M. Knoll, J. Lahann, S. Bräse, *Chem. Soc. Rev*., **2018**, *47*, 6947–6963; b) K. Yoshida, R. Yasue, *Chem. Eur. J*. **2018**, *24*, 18575-18586.

[18] The multinuclear Ag complexes readily decomposed during HPLC techniques, probably because the Ag–N bonds are unstable under the conditions.

[19] J. A. Raskatov, A. L. Thompson, A. R. Cowley, T. D. W. Claridge, J. M. Brown, *Chem. Sci*, **2013**, *4*, 3140-3147.

[20] a) M. Deng, N. F. M. Mukthar, N. D. Schley, G. Ung, *Angew. Chem. Int. Ed*. **2020**, *59*, 1228-1231; b) J.-G. Yang, K. Li, J. Wang, S. Sun, W. Chi, C. Wang, X. Chang, C. Zou, W.-P. To, M.-D. Li, X. Liu, W. Lu, H.-X. Zhang, C.-M. Che, Y. Chen, *Angew. Chem. Int. Ed*. **2020**, *59*, 6915-6922; c) E. S. Gauthier, L. Abella, N. Hellou, B. Darquié, E. Caytan, T. Roisnel, N. Vanthuyne, L. Favereau, M. Srebro-Hooper, J. A. G. Williams, J. Autschbach, J. Crassous, *Angew. Chem. Int. Ed*. **2020**, *59*, 8394-8400; d) T. Ono, K. Ishihama, A. Taema, T. Harada, K. Furusho, M. Hasegawa, Y. Nojima, M. Abe, Y. Hisaeda, *Angew. Chem. Int. Ed*. **2021**, *60*, 2614-2618.

[21] a) J. Kumar, T. Kawai, T. Nakashima, *Chem. Commun*., **2017**, *53*, 1269-1272; b) Z. Han, X.-Y. Dong, P. Luo, S. Li, Z.-Y. Wang, S.Q. Zang, T. C. W. Mak, *Sci. Adv*., **2020**, *6*, eaay0107.

COMMUNICATION

Precious metal sandwiches: New types of multinuclear sandwich complexes consisting of an Ag_3 core and Pt complex units are reported. The first observation of CD and CPL properties from a multinuclear sandwich complex was achieved after optical resolution using a chiral anion.

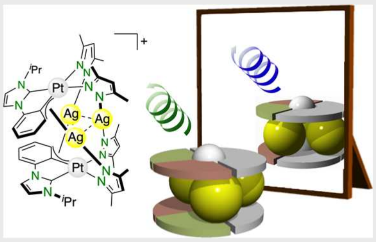

Shinnosuke Horiuchi, Sangjoon Moon, Jacopo Tessarolo, Akitaka Ito, Eri Sakuda, Yasuhiro Arikawa, Guido H. Clever, Keisuke Umakoshi**

Page No. – Page No.

Multinuclear Ag Clusters Sandwiched by Pt Complex Units: Fluxional Behavior and Chiral-at-Cluster Photoluminescence